



HAL
open science

Photodegradation of benzisothiazolinone: Identification and biological activity of degradation products

Zsuzsanna Varga, Edith Nicol, Stéphane Bouchonnet

► To cite this version:

Zsuzsanna Varga, Edith Nicol, Stéphane Bouchonnet. Photodegradation of benzisothiazolinone: Identification and biological activity of degradation products. *Chemosphere*, 2020, 240, pp.124862. 10.1016/j.chemosphere.2019.124862 . hal-02429583

HAL Id: hal-02429583

<https://hal.science/hal-02429583>

Submitted on 21 Dec 2021

HAL is a multi-disciplinary open access archive for the deposit and dissemination of scientific research documents, whether they are published or not. The documents may come from teaching and research institutions in France or abroad, or from public or private research centers.

L'archive ouverte pluridisciplinaire **HAL**, est destinée au dépôt et à la diffusion de documents scientifiques de niveau recherche, publiés ou non, émanant des établissements d'enseignement et de recherche français ou étrangers, des laboratoires publics ou privés.



Distributed under a Creative Commons Attribution - NonCommercial 4.0 International License

1 **Photodegradation of benzisothiazolinone: identification and biological** 2 **activity of degradation products**

3 Zsuzsanna Varga, Edith Nicol and Stéphane Bouchonnet*

4 Laboratoire de Chimie Moléculaire – CNRS / Ecole polytechnique, Institut Polytechnique de
5 Paris – 91128 Palaiseau, France

6

7 **1. Introduction**

8 1,2-benzisothiazol-3(2H)-one (referred to as benzisothiazolinone or BIT, is an antimicrobial
9 agent used as a preservative in mainly aqueous-based chemical chemicals. Banned from
10 cosmetic products, BIT can be found in paints, lacquers, polishes, printing inks, emulsions,
11 cleaning agents, disposable gloves; it is also widely used as a preservative for pesticides
12 ([Schwensen et al., 2015](#); [Rafoth et al. 2007](#); [Flyvholm, 2005](#); [Aalto-Korte et al., 2007](#)). Due to
13 environmental considerations, water-based paints recently replaced solvent-based paints,
14 which require the addition of biocides; isothiazolinones are widely used for this purpose
15 ([Amsler et al., 2017](#)). BIT is also used in paper-based jointing but it degrades during sunlight
16 exposure losing its biocidal efficiency ([Lugg, 2001](#)).

17 Isothiazolinone-type biocides act against various fungi and bacteria by the active sulfur
18 moiety able to oxidize thiol functional groups to form disulfides (e.g. with cysteine) ([Collier](#)
19 [et al., 1990](#)). Besides the biocidal effects on unwanted compounds by reacting with
20 intracellular sulfur-containing proteins ([Collier et al., 1990](#); [Morris et al., 1984](#)),
21 isothiazolinones have also lethal effects on living organisms, the median lethal concentration
22 (LC50) of BIT for zebrafish embryos being 1.03 mg/L ([Li et al., 2016](#)). Growth inhibition

23 effect on *Escherichia coli* and *Schizosaccharomyces pombe* was measured; this inhibitory
24 activity was quenched by thiol-containing materials (glutathione, cysteine), confirming the
25 mechanism of interaction (Collier et al., 1990). According to the European Chemicals
26 Agency, BIT is very toxic to aquatic life, causes eye damage and skin irritation (ECHA,
27 2019). Toxicity tests on zebrafish embryos were performed during ozonation processes and a
28 decrease was found in the overall toxicity of the mixture, due to oxidation of the reductive
29 sulfur in the parent compound (Li et al., 2016). BIT is a developmental toxicant in rats but
30 shows negative mutagenicity (USEPA, 2005). Isothiazolinones were shown to cause severe
31 contact dermatitis and allergy in humans mainly with a high level of occupational exposure
32 (Bregnbak et al., 2013; Bang Pedersen, 1976).

33 It has been shown that isothiazolinones degrade rapidly in soil (Bollmann et al., 2017).
34 Indeed, BIT is easily degraded in the environment but there is no extensive study on the
35 structure of its transformation products, their persistence, and their toxicity. Conventional
36 wastewater treatment plant efficiently removes isothiazolinones at low concentrations (Rafoth
37 et al., 2007). In reverse-osmosis (RO) wastewater treatment plants, BIT is used thanks to its
38 compatibility and non-oxidizing nature and it prevents biofilm growth on membranes (Tang et
39 al., 2012). Nevertheless, studies demonstrated that some isothiazolinones increase the
40 genotoxicity of the RO concentrates (Tang et al., 2013). BIT is added at high concentrations
41 (around 160 mg/l) for which the removal efficiencies of existing approaches are low;
42 ozonation was proposed as an efficient way to degrade BIT (Li et al., 2016). Considering the
43 photochemical degradation, the kinetics was studied under irradiation with a low-pressure
44 UV-C lamp. The process was described to follow pseudo-first order kinetics. Radical species
45 quenching studies were carried out, where the photodegradation of BIT was concluded to be
46 both direct, due to UV absorbance of BIT and indirect, induced by radical oxygen species
47 formation, a widespread mechanism of micropollutant photodegradation (Wang et al., 2017).

48 Different analytical methods were developed for the quantitation of BIT in various matrices.
49 Ultrasonic assisted extraction combined with LC-MS was used to determine BIT at 9.9 mg/kg
50 in hygienic consumer products, specifically in liquid detergents (Heo et al., 2019). BIT was
51 analyzed by matrix solid-phase dispersion followed by LC-MS/MS in household products
52 where it is used as a substitute to chlorinated isothiazolinone; it was found at quite high
53 concentrations in laundry detergent (0.0255% w/w), surface cleaner cream (0.0116 %w/w)
54 and liquid surface cleaner (0.00377% w/w) (Alvarez-Rivera et al., 2012). BIT was found in
55 94% of 47 paints analyzed by LC-MS at concentrations ranging from 28.6 to 1110.74 ppm.
56 These analyses also showed that these products were sometimes labeled incorrectly, e.g. one
57 paint labeled “preservative-free” contained BIT at 71.5 ppm (Goodier et al., 2018).
58 Isothiazolinones were monitored and not detected in environmental waters using
59 derivatization of BIT followed by pre-concentration and GC-MS analysis, with limits of
60 detection ranging from 0.01 to 0.1 µg/L (Rafoth et al., 2007).
61 This work aimed at performing accurate structural elucidation of the photodegradation
62 products of BIT using chromatography and tandem mass spectrometry approaches.
63 Benzisothiazolinone was degraded using two different types of photoreactors in water.
64 Structural elucidation of BIT photoproducts allowed to suggest a coherent degradation
65 pathway on one hand, and to carry out *in silico* toxicity tests to estimate the toxicity of the
66 photoproducts on another hand.

67

68 **2. Materials and methods**

69 *2.1. Chemicals, reagents and sample preparation*

70 1,2-benzisothiazol-3(2H)-one (CAS: 2634-33-5), benzamide, salicylamide, 4-
71 hydroxybenzamide and chromatography grade solvents: acetonitrile (ACN), methanol,
72 dichloromethane and formic acid (FA) were purchased from Sigma Aldrich (Saint-Quentin-
73 Fallavier, France). A Purelab Chorus 1 water purification system (Veolia, Wissous, France)
74 was used to produce ultra-pure water with a conductance of 18.2 S/cm. BIT solutions were
75 prepared at different concentrations: 5, 10, 25, 50 and 100 ppm in water (solubility 1.1 g/l at
76 20 °C (SCCS, 2012) and in acetonitrile. Some experiments were carried out with degassing of
77 the initial solution using nitrogen bubbling for 30 minutes. Different irradiation times were
78 tested to determine the appearance order of photoproducts. Solutions were irradiated for 6
79 hours. Sampling was carried out every 10 minutes during the first hour and then every hour
80 until the end. For GC-MS analysis, all samples (ACN solutions and aqueous samples) were
81 dried using an Xcelvap automated evaporation/concentration system (Horizon Technologies,
82 Bullion, France) and 1 ml of dichloromethane was added. For LC-MS measurements, the
83 samples of different BIT starting concentrations were diluted, in a mixture made of 50%
84 ACN, 50% H₂O and 0.1% formic acid to reach a final concentration of 5 ppm. For HRMS
85 analysis in the infusion mode, samples were diluted in a 90% water / 10% ACN / 0.1% FA
86 mixture, for a starting concentration of BIT of 5 ppm. All the samples were stored away from
87 light at 4 °C; HPLC-MS data showed that degradation was negligible under these conditions,
88 in agreement with literature data where the hydrolytic stability of the compound is mentioned
89 (USEPA, 2005).

90 2.2. Irradiation experiments

91 The UV-Vis absorption spectrum of BIT was recorded in the range of 190 to 500 nm, using a
92 6800 UV-Vis Jenway spectrophotometer (Cole-Parmer, Villepinte, France), with a 1 cm
93 length quartz cell. Based on this spectrum, two irradiation setups were used for

94 photodegradation experiments. The photodegradation of BIT was mainly studied by a Philips
95 HPL-N 125W/542 E27 SC high-pressure mercury lamp (France-Lampes, Saint-Cirq, France)
96 with a wavelength range of 200-650 nm, a maximum irradiation wavelength at 254 nm, and a
97 radiation flux of 6200 lm. The setup consisted of one lamp, circularly surrounded by 6 quartz
98 tubes of 120 ml, all of the elements being in a water bath with water circulation so that the
99 reaction temperature was kept below 28 °C. The samples were also irradiated using a Q-sun
100 test chamber Xe-1-B/S (Q-Lab Saarbücken, Germany) equipped with a xenon arc lamp; a
101 natural light filter X-7640 from the same manufacturer has been used for the reproduction of
102 full sunlight spectrum. The lamp power was 1800 W and the irradiation 0.68 W.m⁻² at
103 a black-standard temperature of 55 °C.

104 2.3. GC-MS analysis

105 Gas chromatographic separations were carried out on an Agilent 450-GC instrument equipped
106 with a 60 m “FactorFour VF-Xms” (10% phenyl, 90% methylpolysiloxane) capillary column,
107 with an internal diameter of 0.25 mm and film thickness of 0.25 µm (Agilent Technologies,
108 Les Ulis, France), coupled with an Agilent 240-MS ion trap mass spectrometer. Samples were
109 injected in splitless mode using an Agilent CP-8400 autosampler, the injection volume was
110 1µl and injector temperature was 280 °C. A gradient temperature program was used with an
111 initial temperature of 50 °C, held for 0.5 min then increased to 280 °C with a ramp of 10
112 °C/min. The carrier gas was high purity helium, with a flow of 1.4 ml/min. Measurements
113 were carried out in electron ionization and positive chemical ionization using methanol as the
114 reagent gas. The filament emission current was set to 10 µA and automatic gain control was
115 used for all experiments. The electron multiplier voltage was automatically optimized at 2200
116 V for a gain value of 10⁵. In the full scan mode, ions were scanned on the range of m/z 50 to
117 m/z 500. Tandem experiment measurements were performed with an ionization storage level

118 of m/z 35 and an isolation window of 3 m/z , using a resonant waveform type with an
119 excitation storage level of m/z 50 and an excitation amplitude of 0.8 V.

120 2.4. LC-MS analysis

121 LC separations were carried out on an Acquity HPLC system (Waters Technologies,
122 Guyancourt, France) coupled with a SolarixXR FT-ICR mass spectrometer equipped with a
123 9.4 T superconducting magnet (Bruker Daltonics, Bremen, Germany). A Pursuit XR^{Ultra} C18
124 column (2.8 μm x 50 mm x 2 mm) (Agilent Technologies, Les Ulis France) was used in
125 gradient mode. Water+0.1% FA (solvent A) and acetonitrile+0.1% FA (solvent B) were used
126 as solvents with a flow rate of 0.2 ml/min. The gradient started at 95% of solvent A for 3 min,
127 then changed linearly to 50% of solvent A in 9 min and then to 5% of solvent A after 12 min
128 of LC run. It was kept at 5% of solvent A for 5 minutes and then set back to the initial
129 percentage of solvent A (95%) for 5 min of equilibrium. An electrospray ionization source
130 was used in both positive and negative modes with a sample flow of 200 $\mu\text{L}/\text{min}$. for both
131 positive and negative mode the nebulizer and drying gas was nitrogen with a flow of 8 L/min
132 at 250 °C for drying gas and 1 bar for nebulizer gas. The capillary voltage was set at - 4500 V
133 and 4000 V in both positive and negative modes, respectively; the spray shield was set at –
134 500 V. The detection mode was broadband with a 4 Mpt resolution in the range of 57.5 to 700
135 m/z with a data reduction of noise of 95%. For tandem MS experiments, precursor ions were
136 isolated with an isolation window of 1 m/z and dissociated with collision energies of 10, 15,
137 20 and 25 V to study the fragmentation mechanisms. In direct infusion mode, the flow rate
138 was 120 $\mu\text{L}/\text{h}$. The spectra were acquired with 4 M data points on a range of 57.7 to 1000
139 m/z . Accumulation time was set to 0.02 s. 100 scans were recorded for each spectrum. The
140 Bruker DataAnalysis software was used to process the chromatograms and spectra.

141 2.5. *In silico* bioassays

142 Preliminary toxicity assessments were performed using the T.E.S.T. software developed by
143 the US Environmental Protection Agency (EPA). This software incorporates different
144 endpoints and approaches, with various individual predictions. The different individual
145 approaches include hierarchical clustering, the Food and Drug Administration (FDA) method,
146 single model, group contribution and nearest neighbor. (Martin, 2016) The reliability of the
147 results in the T.E.S.T. software should be assessed based on the capability of each individual
148 prediction to calculate the toxicity values and then study concordance of the results. A
149 complete description of T.E.S.T. and the included methods can be found on the EPA website
150 (Martin, 2016). Different QSAR methodologies are available to model mutagenicity. The
151 biological testing background of most of them, including T.E.S.T., is the Ames test, which is
152 based on a bacterial mutation of Salmonella typhimurium, reverting the bacteria from
153 histidine dependence to histidine independence (Mortelmans and Zeiger, 2000). The
154 correlation between carcinogenicity in animals and positive mutagenicity in the Ames test
155 was found to be high (Hengstler and Oesch, 2001). The QSAR models for mutagenicity of the
156 compounds of interest were found to be generally of high reliability.

157

158 **3. Results and discussion**

159 *3.1. Physicochemical analysis and photoproducts structural elucidation*

160 The UV/Vis absorption spectrum of BIT shows a high absorbance in the UV region and an
161 additional absorption band with a maximum at 319 nm (see [Supplementary material, Fig. S1](#)).
162 The photodegradation was evidenced by the decrease of the molecule's absorption bands
163 according to time ([Fig. 1](#)). A strong decrease in concentration can be observed during the first

164 15 minutes of irradiation, whereas the degradation slows down later on. This is in good
165 agreement with the exponential decrease evidenced by LC-MS experiments (see below).

166 *Fig. 1*

167 Whatever the chromatograph, using chromatography introduces some subjectivity in the
168 detection process. Actually, the choice of stationary and mobile phases induces some
169 selectivity regarding elution and thus detection of molecules. Therefore, direct infusion MS
170 was used prior to LC-MS coupling, to carry out non-targeted investigation of transformation
171 products in ESI-HRMS. The irradiated solutions were analyzed in both positive and negative
172 modes for the same reasons. The ions detected in direct ESI-HRMS were the same as those
173 detected in LC-MS. Retention times in LC-MS and GC-MS couplings, appearance times of
174 photoproducts during the irradiation process, exact m/z values of $[M+H]^+$ and $[M-H]^-$ ions
175 and corresponding formulae are listed in [Table 1](#). Exact m/z values and corresponding
176 formulae of collision-induced product ions from $[M+H]^+$ or $[M-H]^-$ ions are given in
177 [Supplementary material, Table S1](#).

178 *Table 1*

179 PP1 is among the first appearing photoproducts. It is eluted at 19.3 min in GC-MS; it has the
180 same mass as the parent compound (eluted at 17.8 min) and its EI mass spectrum shows a
181 very similar fragmentation pattern. Its exact formula (C_7H_5NOS) has been determined by HR-
182 MS and confirmed that PP1 corresponds to an isomer of BIT. 1,3-benzothiazol-2(3H)-one
183 was postulated on the basis of PP1 mass spectrum. It was synthesized (the synthesis protocol
184 is reported in [Supplementary material S1](#)) and analyzed using GC-MS; both its retention time
185 and EI mass spectrum confirmed that PP1 corresponds to 1,3-benzothiazol-2(3H)-one ([Table](#)
186 [1](#)). Light-induced isomerization of BIT has been reported in an old study in which three

187 possible isomerization mechanisms were postulated but none was demonstrated (Darlage,
188 1971). Considering the rapid isomerization of BIT into PP1, consequent oxidation processes
189 will have to be considered from both isomers.

190 Three photoproducts (referred as PP2a, PP2b, and PP2c) were detected with retention times of
191 5.4, 6.9 and 8.3 min in LC-MS coupling. They all have a molecular weight of 167 (confirmed
192 by both EI and CI mass spectra in GC-MS) and have been assumed to result from oxygen
193 addition onto the parent compound. For the first one, the concerted losses of CO and SO (m/z
194 168.01196 \rightarrow m/z 96.04471 in CID measurements, Table S1) from the protonated molecule
195 allowed to conclude that the oxygen atom was added onto the sulfur one. The fact that the
196 nitrogen atom was retained in the m/z 96.04471 product ion permitted to conclude in favor of
197 the structure depicted in Table 1, which results from oxidation of PP1 (and not from BIT).
198 Both other PP2 isomers appear after 3 h of irradiation; they display exactly the same CID
199 dissociation pathways. Eliminations of HNC \cdot O and HS \cdot from protonated molecules show that
200 the oxygen atom has been added on the aromatic ring. Hydroxylation of aromatic rings under
201 UV-Vis irradiation has been widely reported in the literature (Matsuura et al., 1974; Kinani et
202 al., 2016). Because it can play an important role regarding toxicity, the exact position of the
203 hydroxyl group has been determined based on CID experiments as depicted in Fig. S2. All the
204 possible structures resulting from hydroxyl addition on the aromatic ring either from BIT or
205 PP1 have been considered in a systematic way: only two of them can undergo two
206 consecutive eliminations of carbon monoxide from the protonated species in positive ESI;
207 their formulae are presented in Table 1.

208 The photoproduct referred as PP3 appears after only 10 min of irradiation. Its exact formula
209 corresponds to the addition of two oxygen atoms on BIT or PP1. In CID experiments, the
210 elimination of SO $_2$ from the deprotonated species (m/z 181.99191 \rightarrow m/z 118.02998, Table

211 S1) leaves no doubt that both oxygen atoms have been added to the sulfur atom. Three
212 mechanisms could be responsible for the formation of PP3: straight addition of a dioxygen
213 molecule onto the sulfur atom from either BIT or PP1, or oxidation of PP2a. As this
214 photoproduct is no more observed when irradiating a degassed solution, it can be concluded
215 in favor of direct dioxygen addition on the sulfur atom. CID results do not permit to
216 discriminate between oxidation of either BIT or PP1 but the structures elucidated for PP4 to
217 PP8 photoproducts are strongly in favor of BIT oxidation, as discussed in the next section. It
218 is to be noted that the structure suggested for PP3 corresponds to saccharin, which has been
219 proved to be an oxidation product of BIT in a study dedicated to BIT ozonation (Li et al.,
220 2016).

221 PP4 has been detected in negative ESI, at a very short retention time (1.2 min) in reverse-
222 phase chromatography suggesting a highly polar structure. Its mass spectrum exhibits a major
223 ion resulting from deprotonation of the molecule. For these reasons, the structure suggested
224 for PP4 in Table 1 includes a SOOH group, which allows easy removal of a proton in
225 negative ESI. The SO₂ elimination in CID experiments is in good agreement with the
226 proposed structure.

227 PP5 has been detected in both positive and negative ESI. Its elemental composition
228 corresponds to that of PP4 plus a hydroxyl group. In the negative mode, observation of the
229 deprotonated molecule indicates an acidic function (in agreement with the short eluting time
230 in LC-MS). In the positive mode, the consecutive losses of ammonia and SO₂ imply that the
231 amido function has been kept and that the sulfur atom carries two oxygen atoms. This implies
232 that the additional hydroxyl group is bound to the aromatic ring. It has been located in ortho
233 position with regard to the amido function since the formation of both PP2b and PP2c
234 photoproducts shows that hydroxylation in this position is favored over additions onto other

235 positions of the ring. The consecutive losses of SO₂ and H₂O from [PP5 - H]⁻ in CID
236 experiments (m/z 200.00250 → m/z 118.02997) confirm this hypothesis (see the dissociation
237 pathways of [PP5 - H]⁻ in [Fig. S3](#)).

238 Three photoproducts referred as PP6a to PP6c were detected at short retention times (between
239 0.9 and 2.3 min) in negative ESI. Their exact formulae correspond to the addition of an
240 oxygen atom onto PP5. In CID experiments, the isomer eluting at 0.9 min undergoes losses of
241 NH₃ and O=C=NH indicating that it still has the amido function; it demonstrates that the
242 aromatic ring has been hydroxylated. The ammonia elimination, barely observed in negative
243 ESI, has to be charge-induced. By analogy with other photoproducts and to rationalize the
244 NH₃ loss (see [Fig. S4](#)), the hydroxyl group was assumed to be in ortho position relative to the
245 amido group. In the negative mode, the losses of HCNO and SO₂ from [PP6b - H]⁻ indicate
246 that two hydroxyl groups are carried by the aromatic ring in the PP6b structure.
247 Unfortunately, CID experiments provided too few ions to allow the location of these
248 hydroxyl groups. Both losses of HCNO₂ and SO₃ from [PP6c - H]⁻ allowed the easy
249 determination of the PP6c structure, as depicted in [Fig. S4](#).

250 PP7 has been easily identified as benzamide based on GC-MS and LC-MS analysis of the
251 corresponding standard. As for PP7, PP8 isomers (PP8a to PP8c, see [Table 1](#)) were easily
252 identified since salicylamide and 4-hydroxybenzamide were commercially available and were
253 used to check mass spectra and retention times in GC-MS.

254 *3.2. Mechanistic approach of BIT photodegradation*

255 The photodegradation of BIT and the appearance of photoproducts were monitored using LC-
256 MS in both positive and negative modes, at various concentrations ranging from 5 to 100
257 ppm. The detected photoproducts were the same regardless the initial BIT concentration,

258 although the reaction kinetics slightly differed, the photodegradation being slower at higher
259 concentrations, as displayed in [Supplementary material, Fig. S5 and S6](#). At 5 ppm, BIT is
260 undetectable after 30 minutes of irradiation while the initial amount of BIT has been reduced by
261 60% at 100 ppm for the same irradiation time. For each photoproduct, [Table 1](#) gives the time
262 at which it is first detected and the time at which it is no longer detected. Based on the
263 kinetics of the appearance and disappearance of photoproducts, stepwise photodegradation
264 mechanisms were proposed ([Fig. 2](#)). Structures between brackets were not observed, likely
265 because of too short lifetimes. It is to be noted that the formation of sulfite ions, reported by a
266 previous study, was not evidenced in the present work but is in good agreement with the
267 observed decrease of the mixture pH ([Li et al., 2016](#)).

268 [Fig. 2](#)

269 Isomerization of BIT into PP1 is very fast; it is not possible to state if this isomerization is
270 partially reversible. Isomerization of other compounds including five-membered ring
271 structures (PP2 isomers) could also not be established but could explain the formation of PP4
272 from PP2a (see [Fig. 2](#)). From BIT or PP1, the formation of all the photoproducts can be
273 rationalized by successive or competitive mechanisms including direct oxygen addition onto
274 the sulfur atom (so that it reaches its highest oxidation state), hydroxyl addition, hydrolysis,
275 and SO₃ elimination. The comparison of results between degassed and non-degassed solutions
276 showed that the same photoproducts are produced in both cases. They are less abundant in
277 degassed solutions, for which BIT dimers are also observed. This is likely because a reduced
278 concentration in oxygen disfavors mechanisms involving dissolved oxygen and thus favors
279 intermolecular reactions between BIT excited species.

280 *3.3. In silico toxicity estimations*

281 For each photoproduct, QSAR results on mutagenicity, oral rat and Fathead minnow toxicity
282 were considered to be compared to that of the parent compound. The results of *in silico*
283 *toxicity* estimations are summarized in Table 2. Since the structure of PP6b was not accurately
284 determined (the position of the second hydroxyl group on the aromatic ring could not be
285 stated, see Table 1), toxicity estimation could not be performed on this compound. Regarding
286 mutagenicity, T.E.S.T. works with a dataset of 5743 chemicals and provides a binary result
287 (positive/negative). Experimental values were provided by the software for BIT, PP3, PP7,
288 and PP8a; they were all in accordance with the calculated results. *In silico* estimations showed
289 non-mutagenicity for all the photoproducts except PP4. For this compound, only 2 out of 3
290 individual predictions provided any result and both results were contradictory, therefore the
291 mutagenicity positive result for PP4 is of low reliability; it might be a false positive result and
292 should be treated accordingly. Fathead minnow LC₅₀ (96 h), represents the concentration that
293 kills half of the fish population (*Pimephales promelas*) in 4 days. The training set was
294 obtained from the ECOTOX database, with a dataset containing 823 chemicals. The parent
295 compound showed to be the most toxic but LC₅₀ values could not be estimated for PP1, PP2b,
296 PP3, and PP6c: none of the individual models provided a result since the requirements for
297 reliable toxicity assessment were not fulfilled for these compounds. For PP8a (salicylamide)
298 the proposed experimental toxicity value was in good agreement with the calculated one but
299 for PP7, for which an experimental result was also available, the experimental value was 3.5
300 times higher than the calculated one. The oral rat LD₅₀ endpoint gives the amount of
301 chemical, in terms of the mass of the chemical over weight of the rat, which kills half of the
302 rats when orally ingested. In this case, the ChemIDplus database was used to calculate
303 toxicity data of interest with a final dataset of 7413 chemicals. For this endpoint, there was no
304 prediction for photoproduct PP6a but the others proved to be of high reliability. Experimental
305 values showed good accordance with the calculated ones for the parent compound.

306 Photoproducts PP2a, PP2c, PP4, PP5, PP8b, and PP8c exhibited slightly higher or similar
307 toxicity as the parent compound. Compound PP5 fell into the moderately toxic category (50-
308 500 mg/kg) on the Hodge and Sterner scale (Hodge and Sterner, 1949). All the other
309 compounds were categorized as slightly toxic. For PP8a different oral rat toxicity values were
310 reported in the literature but generally, the experimental values were approximately 2 times
311 lower, closer to the toxicity values determined for PP8b and PP8c (Table 2) (Goldenthal,
312 1971; Boxill et al., 1958). It could explain the discrepancy among the PP8 compound family,
313 in which photoproducts display isomeric structures. Given that oral rat toxicity calculations
314 proved to be of adequate reliability, toxicophores of the critical compounds are further
315 discussed. The potential toxicity of PP2a cannot be compared to those of other compounds
316 since its structure includes a very specific and uncommon –SO-CO-NH- structure (Table 1). It
317 is interesting to note that, at the exception of PP2a, all the photoproducts exhibiting potential
318 toxicity include either a phenolic (PP2c, PP8b and PP8c) or sulfino (-SO₂H) group (PP4).
319 Furthermore, the most toxic compound (PP5) is the one including both functions. The toxicity
320 of phenolic compounds has been widely reported but that of the sulfino group is not discussed
321 in the literature, therefore no conclusion could be drawn but it might be interesting to
322 investigate further this class of compounds.

323 *Table 2*

324 **4. Conclusion**

325 The UV-VIS irradiation of an aqueous solution of benzisothiazolinone led to the formation of
326 fourteen photoproducts, their chemical structures were elucidated based on GC-MS, LC-
327 MS/MS, and FT-ICR-MS experiments. Based on the chemical structures determined and their
328 appearance order, a photo induced-degradation mechanism of benzisothiazolinone was
329 proposed, which combines isomerization, oxidation, hydroxylation, hydrolysis, and

330 elimination processes. Regarding to toxicity estimations, the absence of mutagenicity of
331 photoproducts and the moderate oral rat LD₅₀ values determined for some of them (while
332 most of them are less toxic than the parent compound) leads to consider direct
333 photodegradation as a potential powerful tool to remove benzisothiazolinone, even when it is
334 used in large amounts in some wastewater treatment plants. This is even more interesting
335 considering that these photoproducts were not persistent after a few hours of UV-light
336 irradiation.

337

338 **Acknowledgments**

339 We are very thankful to Dr Gregory Danoun, Researcher at the LCM, who performed the
340 synthesis of BIT.

341 This work is part of a project that has received funding from the European Union's Horizon
342 2020 research and innovation program under the Marie Skłodowska-Curie Grant Agreement
343 No 765860 (AQUALity). Financial support from the National FT-ICR network
344 (FR3624CNRS) and from the Ile de France Région are also gratefully acknowledged.

345

346 **References**

- 347 Aalto-Korte, K., Ackermann, L., Henriks-Eckerman, M.-L., Valimaa, J., Reinikka-Railo, H.,
348 Leppanen, E., Jolanki, R. (2007). **1,2-Benzisothiazolin-3-one in disposable polyvinyl**
349 **chloride gloves for medical use.** *Contact Derm.*, 57(6), 365–370
- 350 Alvarez-Rivera, G., Dagnac, T., Lores, M., Garcia-Jares, C., Sanchez-Prado, L., Lamas, J.P.,
351 Llompart, M. (2012). **Determination of isothiazolinone preservatives in cosmetics**
352 **and household products by matrix solid-phase dispersion followed by high-**
353 **performance liquid chromatography-tandem mass spectrometry.** *J. Chromatogr. A*,
354 1270, 41–50
- 355 Amsler, E., Aerts, O., Raison-peyron, N., Debons, M., Milpied, B., Giordano-labadie, F.,
356 Barbaud, A. (2017). **Airborne allergic contact dermatitis caused by isothiazolinones**
357 **in water-based paints : a retrospective study of 44 cases.** *Contact Derm.*, 77(3), 163–
358 170
- 359 Bang Pedersen, N. (1976). **Occupational allergy from 1,2-benzisothiazolin-3-one and**
360 **other preservatives in plastic emulsions.** *Contact Derm.*, 2(6), 340–342
- 361 Bollmann, U. E., Fernández-calviño, D., Koefoed, K., Storgaard, M.S., Sanderson, H., Bester,
362 K. (2017). **Biocide runoff from building facades: Degradation kinetics in soils.**
363 *Environ. Sci. Technol.*, 51(7), 3694–3702
- 364 Boxill, B.G.C., Nash, C.B., Wheeler, A.G. (1958). **Comparative pharmacological and**
365 **toxicological evaluation of N-Acetyl-p-aminophenol, salicylamide, and**
366 **acetylsalicylic acid.** *J. Am. Pharm. Assoc.*, 47(7), 479–487
- 367 Bregnbak, D., Lundov, M.D., Zachariae, C., Menné, T., Johansen, J.D. (2013). **Five cases of**
368 **severe chronic dermatitis caused by isothiazolinones.** *Contact Derm.*, 69(1), 57–59
- 369 Collier, P.J., Ramsey, A.J., Austin, P., Gilbert, P. (1990). **Growth inhibitory and biocidal**
370 **activity of some isothiazolonone biocides.** *J. Appl. Bacteriol.*, 69(4), 569–577

371 Darlage, L.J. **Thermal, photochemical, and electron impact induced transformations of**
372 **1,2-benzisoxazolin-3-ones and related heterocyclic compounds.** Iowa State
373 University, Iowa, USA (1971)

374 European Chemicals Agency. (2019). **1,2-benzisothiazol-3(2H)-one.**
375 <https://echa.europa.eu/substance-information/-/substanceinfo/100.018.292>

376 Flyvholm, M.-A. (2005). **Preservatives in registered chemical products.** Contact Derm., 53,
377 27–32

378 Goldenthal, E.I. (1971). **A Compilation of LD50 values in newborn and adult animals.**
379 Toxicol. Appl. Pharmacol., 18, 185–207

380 Goodier, M.C., Siegel, P.D., Zang, L., Warshaw, E.M. (2018). **Isothiazolinone in residential**
381 **interior wall paint: a high-performance liquid chromatographic – mass**
382 **spectrometry analysis.** Am. J. Contact Dermatitis, 29(6), 332–338

383 Hengstler, J.G., Oesch, F. (2001). **Ames Test.** Encyclopedia of Genetics (pp. 51–54).
384 <https://doi.org/10.1006/rwgn.2001.1543>

385 Heo, J.J., Kim, U., Oh, J. (2019). **Simultaneous quantitative analysis of four**
386 **isothiazolinones and 3-iodo-2-propynyl butyl carbamate present in hygienic**
387 **consumer products.** Environ. Eng. Res., 24(1), 137–143

388 Hodge, H.C., Sterner, J.H. (1949). **Tabulation of Toxicity Classes.** Am. Ind. Hyg. Assoc. J.,
389 10(4), 93–96

390 Kinani, S., Souissi, Y., Kinani, A., Vujović, S, Aït-Aïssa, S., Bouchonnet, S. (2016).
391 **Photodegradation of fluorene in aqueous solution: Identification and biological**
392 **activity testing of degradation products.** J. Chromatogr. A, 1442, 118-28

393 Li, A., Chen, Z., Wu, Q.Y., Huang, M.H., Liu, Z.Y., Chen, P., Mei, L.-C., Hu, H.Y. (2016).
394 **Study on the removal of benzisothiazolinone biocide and its toxicity: the**
395 **effectiveness of ozonation.** Chem Eng J, 300, 376–383

396 Lugg, M.J. (2001). **Photodegradation of the biocide 1, 2-benzothiazolin-3-one used in a**
397 **paper-based jointing material.** *Int. Biodeterior. Biodegradation*, 48(1–4), 252–254

398 Martin, M.T. (2016). **User’s Guide for T.E.S.T. (version 4.2) (Toxicity Estimation**
399 **Software Tool).**
400 <https://www.epa.gov/chemical-research/toxicity-estimation-software-tool-test%0AUser’s>

401 Morris, S.L., Walsh, R.C., Hansenq, J.N. (1984). **Identification and characterization of**
402 **some bacterial membrane sulfhydryl groups which are targets of bacteriostatic and**
403 **antibiotic action.** *J. Biol. Chem.*, 259(21), 13590–13594.

404 Mortelmans, K., Zeiger, E. (2000). **The Ames Salmonella/microsome mutagenicity assay.**
405 *Mutat. Res.*, 455(1–2), 29–60

406 Rafoth, A., Gabriel, S., Sacher, F., Brauch, H.J. (2007). **Analysis of isothiazolinones in**
407 **environmental waters by gas chromatography-mass spectrometry.** *J. Chromatogr. A*,
408 1164(1–2), 74–81

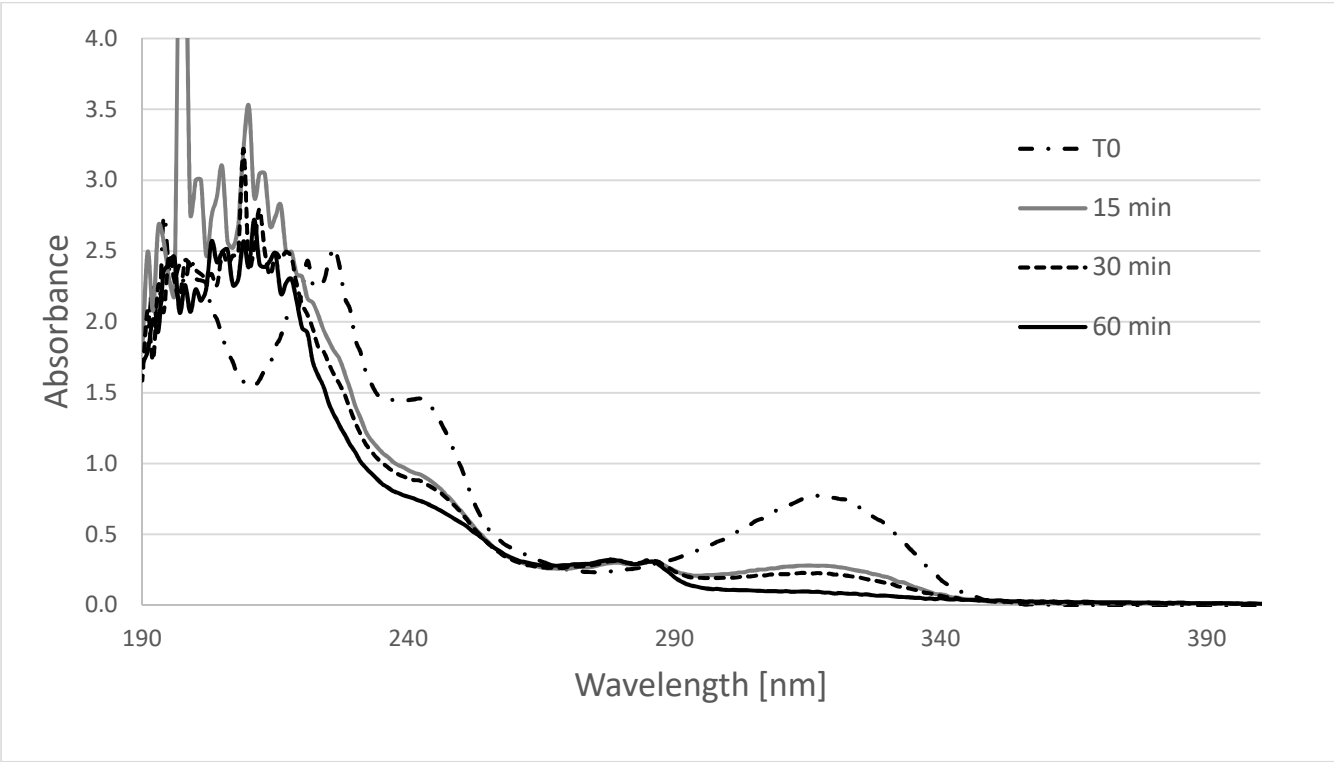
409 SCCS (Scientific Committee on Consumer Safety), **Opinion on benzisothiazolinone**, 26-27
410 June 2012.
411 https://ec.europa.eu/health/scientific_committees/consumer_safety/docs/sccs_o_099.pdf

412 Schwensen, J.F., Lundov, M.D., Bossi, R., Banerjee, P., Gimenez-Arnau, E., Lepoittevin, J.P.,
413 Liden, C., Uter, W., Yazar, K., White, I.R., Johansen, J.D. (2015).
414 **Methylisothiazolinone and benzisothiazolinone are widely used in paint: a**
415 **multicentre study of paints from five European countries.** *Contact Derm.*, 72(3),
416 127–138

417 Tang, F., Sun, Y.-X., Shi, Y., Li, X., Hu, H.-Y. (2012). **Chemicals consumption and cost**
418 **analysis of a microfiltration-reverse osmosis process for wastewater reclamation.**
419 *China Environ. Sci.*, 32(9), 1613–1619

420 Tang, F., Hu, H., Wu, Q., Tang, X., Sun, Y., Shi, X. (2013). **Effects of chemical agent**

421 **injections on genotoxicity of wastewater in a microfiltration-reverse osmosis**
422 **membrane process for wastewater reuse.** J. Hazard. Mater., 260, 231–237
423 U.S. Environmental Protection Agency. (2005). **Reregistration Eligibility Decision (RED)**
424 **for Benisothiazolin-3-one.**
425 https://archive.epa.gov/pesticides/reregistration/web/pdf/benisothiazolin_red.pdf
426 Wang, T., Wu, Q.Y., Wang, W.L., Chen, Z., Li, B.T., Li, A., Liu, Z.-Y., Hu, H.Y. (2017).
427 **Self-sensitized photodegradation of benisothiazolinone by low-pressure UV-C**
428 **irradiation: kinetics, mechanisms, and the effect of media.** Sep. Purif. Technol., 189,
429 419–424
430



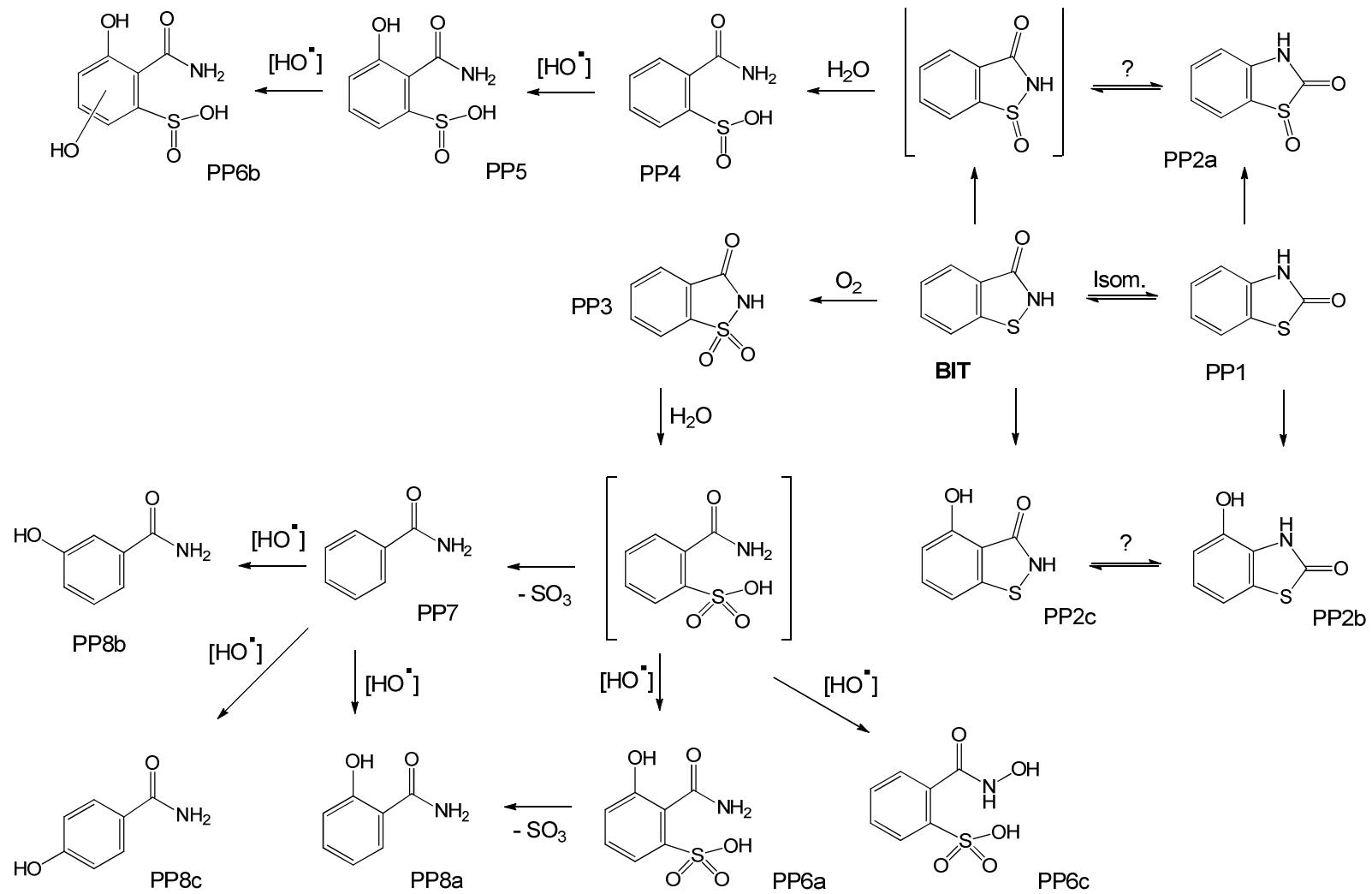
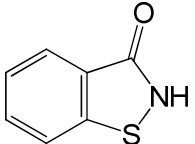
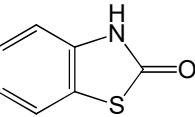
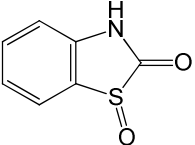
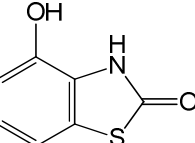
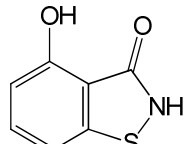
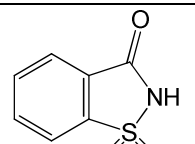
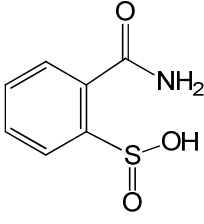
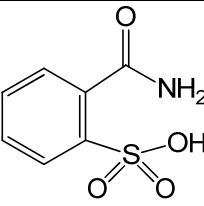
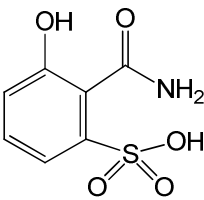
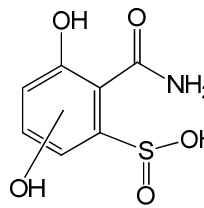
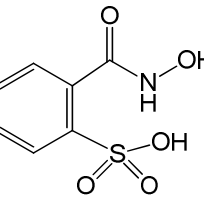
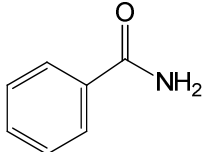


Figure 2. Suggested pathways for the photodegradation of BIT

Table 1. Photoproducts of BIT detected in LC-MS and GC-MS couplings

Compound	Time of first detection (min)	Time when not present anymore (min)	Retention time in LC-MS (min)	Retention time in GC-MS (min)	m/z measured for [M+H] ⁺ in ESI+	m/z measured for [M-H] ⁻ in ESI-	Theoretical mass of the neutral	Empirical formula of the neutral	Chemical structure
BIT	0	120	7.2	17.8	152.01642	150.00203	151.00918	C ₇ H ₅ NOS	
PP1	10	480	9.3	19.3	152.01636	150.00206	151.00918	C ₇ H ₅ NOS	
PP2a	10	120	5.4	20.3	168.01123	165.99698	167.00410	C ₇ H ₅ NO ₂ S	
PP2b	50	420	7.0	-	168.01120	165.99700	167.00410	C ₇ H ₅ NO ₂ S	
PP2c	50	420	8.3	-	168.01122	165.99699	167.00410	C ₇ H ₅ NO ₂ S	
PP3	10	120	3.8	-	-	181.99191	182.99901	C ₇ H ₅ NO ₃ S	

PP4	10	120	1.2	-	168.01123	184.00756	185.01466	C ₇ H ₇ NO ₃ S	
PP5	10	480	1.8	-	202.01665	200.00250	201.00957	C ₇ H ₇ NO ₄ S	
PP6a	30	480	0.9	-	-	215.99742	217.00449	C ₇ H ₇ NO ₅ S	
PP6b	30	480	1.5	-	-	215.99741	217.00449	C ₇ H ₇ NO ₅ S	
PP6c	30	480	2.3	-	-	215.99742	217.00449	C ₇ H ₇ NO ₅ S	
PP7	50	480	5.6	14.9	122.05992	-	121.05276	C ₇ H ₇ NO	

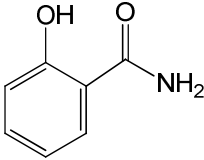
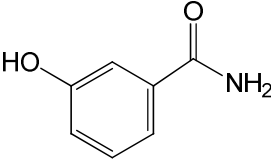
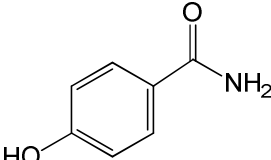
PP8a	50	480	7.3	16.5	138.05482	-	137.04768	C ₇ H ₇ NO ₂	
PP8b	50	480	2.5	-	138.05480	-	137.04768	C ₇ H ₇ NO ₂	
PP8c	50	360	7.1	-	138.05483	-	137.04768	C ₇ H ₇ NO ₂	

Table 2. Toxicity values estimated by the T.E.S.T. software for BIT and its photoproducts except PP6b

Compounds	Mutagenicity (Ames test)	Fathead minnow LC50 (96) [mg/L]	Oral rat LD50 [mg/kg]
BIT	Negative	25	894
PP1	Negative	NA ^a	1169
PP2a	Negative	148	527
PP2b	Negative	NA	3235
PP2c	Negative	36	941
PP3	Negative	NA	1685
PP4	Positive	140	649
PP5	Negative	79	412
PP6a	Negative	55	NA
PP6c	Negative	NA	3385
PP7	Negative	186	1123
PP8a	Negative	166	1619
PP8b	Negative	144	897
PP8c	Negative	126	608

NA^a: Non applicable